

Electronic Supplementary Information

Unprecedented thermal condensation of tetracyanocyclopropanes to triazaphenalenenes: a facile route to design of novel materials for electronic applications

Iliya E. Kuznetsov,^a Diana K. Susarova,^a Lyubov A. Frolova,^a Alexander S. Peregudov,^b Alexander F. Shestakov,^a Sergey I. Troyanov,^c Keith J. Stevenson^d and Pavel A. Troshin*^{d,a}

^a IPCP RAS, Semenov Prospect 1, Chernogolovka, 142432, Russia. Fax: +7 496522-3507; Tel: +7 496522 1418; E-mail: troshin2003@inbox.ru.

^b INEOS RAS, Vavylova St. 28, B-334, Moscow, 119991, Russia.

^c Department of Chemistry, Moscow State University, Leninskie gory, Moscow, 119991, Russia

^d Skolkovo Institute of Science and Technology, Nobel St. 3, Moscow, 143026, Russian Federation

Contents

<i>General synthetic procedure for preparation of triazaphenalenenes</i>	3
<i>X-ray crystallography</i>	4
<i>DFT calculations</i>	4
<i>Fabrication and characterization of the OFET-based memory elements using compound 5 as a light-sensitive component</i>	6
<i>Fabrication and characterization of OLEDs based on compound 1</i>	7
<i>Figure S1. ESI mass spectrum of the crude reaction product formed via thermal cyclization of 3-(4-methoxyphenyl)cyclopropane-1,1,2,2-tetracarbonitrile, showing the formation of triazaphenalene 2 as a major (formal dimerization) product along with the unidentified cyclopropane trimerization and tetramerization products.</i>	8
<i>Figure S2. ¹H (a) ¹³C (b) NMR spectra of compound 1 recorded in DMSO-D₆</i>	8
<i>Figure S3. J-mode ¹³C NMR spectrum of compound 1 recorded in DMSO-D₆</i>	10

<i>Figure S4. 2D H-C HSQC NMR spectrum of 1 in DMSO-D₆</i>	10
<i>Figure S5 2D H-C HMBC NMR spectrum of 1 in DMSO-D₆</i>	11
<i>Figure S6. ¹H NMR spectrum of 2 in DMSO-D₆</i>	12
<i>Figure S7. J-mode ¹³C NMR spectrum of 2 in DMSO-D₆</i>	12
<i>Figure S8. ¹H NMR spectrum of 3 in DMSO-D₆</i>	13
<i>Figure S9. ¹³C NMR spectrum of 3 in DMSO-D₆</i>	13
<i>Figure S10. ¹H NMR spectrum of 4 in DMSO-D₆</i>	14
<i>Figure S11. A low-field part of ¹H NMR spectrum of 4 in DMSO-D₆</i>	14
<i>Figure S12. ¹³C NMR spectrum of 4 in DMSO-D₆</i>	15
<i>Figure S13. ¹H NMR spectrum of 5 in DMSO-D₆</i>	16
<i>Figure S14. ¹³C NMR spectrum of 5 in DMSO-D₆</i>	16
<i>Figure S15. ¹H NMR spectrum of 6 in DMSO-D₆</i>	17
<i>Figure S16. ¹³C NMR spectrum of 6 in DMSO-D₆</i>	17
<i>Figure S17. Low-field parts of the ¹H NMR spectra of 1 in CDCl₃ (a) and DMSO-D₆ (b)</i>	18
<i>Figure S18. 2D ¹H-¹⁵N HMBC spectrum of compound 1 in DMSO-D₆</i>	19
<i>Figure S19. Calculated molecular structure of compound 1.</i>	20
<i>Figure S20. Calculated structure of the transition state for rotation of NH₂ group in 1.</i>	20
<i>Figure S21. Absorption and PL spectra of selected triazaphenalenenes in toluene solutions</i>	21
<i>Figure S22. Solid-state absorption spectrum of triazaphenalene 1</i>	22
<i>Figure S23. Calculated structure of the product of cyclization of 1.</i>	22

General synthetic procedure for preparation of triazaphenalenenes

The corresponding 3-arylcyclopropane-1,1,2,2-tetracarbonitrile (2 mmol) was dissolved in 50 mL of 1,2-dichlorobenzene. The obtained solution was heated at reflux for 30-40 h in argon. Then the reaction mixture was cooled down to the room temperature, filtered through a paper filter and the filtrate was concentrated in vacuum using rotary evaporator. The obtained residue was redissolved in toluene and poured on the top of silica gel (Acros Organics, 40–60 μ , 60 Å) column. The target triazaphenalene was eluted toluene-MeOH mixture (99:1 v/v). The product yields ranged from 14 to 57%.

Compound 1. Yield 57%. ^1H NMR (600 MHz, DMSO-D_6) δ = 2.41 (s, 6H), 7.42 (m, 6H), 7.92 (d, 2H, J =8.5 Hz), 8.61 (s, 1H), 9.23 (s, 1H) ppm. ^{13}C NMR (150 MHz, DMSO-D_6) δ = 21.51, 21.69, 73.57, 79.64, 88.14, 89.54, 94.86, 112.97, 114.17, 114.72, 115.55, 127.69, 128.47, 128.65, 129.08, 129.37, 129.9, 129.94, 130.92, 131.49, 141.78, 144.07, 150.21, 152.44, 156.04, 161.35, 162.41, 166.61 ppm. ESI-MS: m/z =463 ($[\text{M-H}]^-$). Cald., %: C, 72.40; H, 3.47, N, 24.12. Found., %: C, 71.95; H, 3.14, N, 23.89. Melting point >240 °C (decomposes).

Compound 2. Yield 29%. ^1H NMR (600 MHz, DMSO-D_6) δ = 3.87 (s, 6H), 7.16 (m, 4H), 7.51 (d, 2H, J =8.7 Hz), 8.10 (d, 2H, J =9.1 Hz), 8.56 (s, 1H), 9.17 (s, 1H) ppm. ^{13}C NMR (150 MHz, DMSO-D_6) δ = 55.92, 56.18, 73.33, 87.74, 88.36, 94.55, 113.09, 114.43, 114.74, 114.84, 115, 115.91, 125.62, 126.26, 129.32, 130.62, 131.18, 131.35, 150.19, 152.18, 156.08, 161.37, 161.85, 162.01, 163.7, 165.48 ppm. ESI-MS: m/z =495 ($[\text{M-H}]^-$). Cald., %: C, 67.74; H, 3.25, N, 22.57. Found., %: C, 67.66; H, 3.31, N, 22.44. Melting point >240 °C (decomposes).

Compound 3. Yield 21%. ^1H NMR (600 MHz, DMSO-D_6) δ = 7.86 (d, 2H, J =8.7 Hz), 8.15 (d, 2H, J =8.7 Hz), 8.45 (m, 4H) 8.84 (s, 1H), 9.46 (s, 1H) ppm. ^{13}C NMR (150 MHz, DMSO-D_6) δ = 74.55, 88.76, 91.92, 94.89, 112.56, 113.63, 114.08, 114.69, 124.52, 124.72, 125.78, 128.67, 129.37, 130.29, 130.41, 137.81, 139.87, 139.92, 149.47, 150.06, 150.17, 152.74, 155.72, 160.75, 161.17, 165.67 ppm. ESI-MS: m/z =525 ($[\text{M-H}]^-$). Cald., %: C, 59.32; H, 1.91, N, 26.61. Found., %: C, 58.98; H, 1.87, N, 26.45. Melting point >240 °C (decomposes).

Compound 4. Yield 28%. ^1H NMR (600 MHz, DMSO-D_6) δ = 1.32 (s, 9H), 1.33 (s, 9H), 7.48 (d, 2H, J =8.7 Hz), 7.63 (m, 4H), 7.93 (d, 2H, J =8.4 Hz), 8.61 (s, 1H), 9.21 (s, 1H) ppm. ^{13}C NMR (150 MHz, DMSO-D_6) δ = 31.23, 31.38, 35.26, 35.43, 73.6, 88.08, 89.64, 94.76, 112.99, 114.22, 114.79, 115.57, 126.17, 126.23, 128.49, 128.96, 129.38, 130.63, 130.8, 131.57, 132.26, 133.05, 150.31, 152.54, 154.56, 156.67, 161.38, 162.18, 166.71, 164.42 ppm. ESI-MS: m/z =547 ($[\text{M-H}]^-$). Cald., %: C, 74.43; H, 5.14, N, 20.42. Found., %: C, 74.68; H, 4.86, N, 20.31. Melting point >240 °C (decomposes).

Compound **5**. Yield 53%. ^1H NMR (600 MHz, DMSO- D_6) δ = 7.50 (m, 2H), 7.87 (m, 6H), 8.68 (s, 1H), 9.29 (s, 1H) ppm. ^{13}C NMR (150 MHz, DMSO- D_6) δ = 73.55, 87.92, 89.97, 94.33, 112.29, 113.45, 113.95, 114.69, 124.93, 126.86, 130.13, 130.41, 132.05, 132.12, 132.5, 132.9, 149.69, 152.07, 155.42, 160.76, 160.92, 165.53 ppm. ESI-MS: m/z =593 ($[\text{M}-\text{H}]^-$). Cald., %: C, 52.55; H, 1.70, N, 18.86. Found., %: C, 52.36; H, 1.54, N, 18.92. Melting point >240 °C (decomposes).

Compound **6**. Yield 14%. ^1H NMR (600 MHz, DMSO- D_6) δ = 7.33 (dd, 1H, J_1 =5.1 Hz, J_2 =3.7 Hz), 7.39 (dd, 1H, J_1 =5.0 Hz, J_2 =4.0 Hz), 7.66 (dd, 1H, J_1 =3.6 Hz, J_2 =1.2 Hz), 8.06 (dd, 1H, J_1 =5.1 Hz, J_2 =1.1 Hz), 8.18 (dd, 1H, J_1 =5.1 Hz, J_2 =1.0 Hz), 8.36 (dd, 1H, J_1 =4.1 Hz, J_2 =1.0 Hz), 8.64 (s, 1H), 9.24 (s, 1H) ppm. ^{13}C NMR (150 MHz, DMSO- D_6) δ = 73.68, 85.81, 87.29, 93.94, 112.94, 114.33, 114.65, 115.61, 128.68, 130.52, 132.43, 132.74, 132.97, 133.61, 137.78, 138.93, 150.22, 152.05, 154.52, 155.65, 158.37, 161.20 ppm. ESI-MS: m/z =447 ($[\text{M}-\text{H}]^-$). Cald., %: C, 58.92; H, 1.80, N, 24.99. Found., %: C, 59.03; H, 1.77, N, 24.71. Melting point >240 °C (decomposes).

X-ray crystallography

Synchrotron X-ray data for a crystal of **1** with dimensions $0.04 \times 0.01 \times 0.01$ mm³ were collected at 100 K on the BL14.2 at the BESSY storage ring (Berlin, Germany) using a MAR225 detector, $\lambda = 0.9050$ Å. $\text{C}_{28}\text{H}_{16}\text{N}_8 \cdot 0.5\text{PhMe} \cdot \text{MeOH}$, triclinic, $P\bar{1}$, $a = 6.7285(2)$, $b = 12.4807(4)$, $c = 17.2061(8)$ Å, $\alpha = 107.9080(13)$, $\beta = 91.5310(15)$, $\gamma = 99.840(2)^\circ$, $V = 1349.83(9)$ Å³, $Z = 2$, $R_1/wR_2 = 0.107/0.282$ for 3360/3686 reflections and 396 parameters. The solvated molecule of toluene is disordered around an inversion center. CCDC 1522029 contains the supplementary crystallographic data for this paper. These data can be obtained free of charge from The Cambridge Crystallographic Data Centre via http://www.ccdc.cam.ac.uk/data_request/cif.

DFT calculations

Theoretical calculations were performed using PBE density functional method (ref. 1) and Λ_2 basis (ref. 2) of cc-pVTZ quality using the PRIRODA program package (ref. 3) at the Joint Supercomputer Center of the Russian Academy of Sciences. Relative energies were calculated taking into account zero-point vibration energies. This approach allowed us to reproduce the geometry of the molecule of compound **1** with a high precision (Fig. S19). The mean absolute deviation of the calculated bond lengths from the experimental ones was in the range of 0.01 Å. The dihedral angles defined by the planes of the triazaphenalene system and phenyl rings were 24 and 51 degrees, thus corresponding well to the experimental values of 20 and 53 degrees. The calculated structure of the transition state for NH_2 group rotation is shown in Fig. S20. A high

value of the activation energy of 80.0 kJ/mol for this rotation is caused by shortening of the C-NH₂ bond in **1** due to the conjugation effects.

It was shown previously (ref. 4) that DFT theory allows one to reproduce well the energy characteristics of tautomers of arylamines. Relative energy of the imine-form with respect to the ground form of 2-aminopyridine calculated by B3LYP/6-311+G** approach is equal to 58.5 kJ/mol (ref. 5) and agrees with the value of 53.6 kJ/mol obtained using PBE/Λ2 approach. The structure of the low energy imine-type tautomer of compound **1** is shown in Fig. S21. It has 68.8 kJ/mol higher energy than the ground form shown in Fig. S19. A similar value of 58.0 kJ/mol was obtained for the imine form of 4-amino-5-cyano-pyrimidine, which also showed significant shortening of the C-NH₂ bond down to 1.348 Å.

In order to assess the effects of solvation, a complex of compound **1** with 2 DMSO molecules was investigated. It has been shown that DMSO binds to the H atoms of the NH₂ group. Solvation induces the elongation of the N-H bonds by 0.005 - 0.068 Å accompanied by shortening of the H...O distances from 2.11 to 1.55 Å. The H₂N-C bond becomes shorter by 0.018 Å due to the aforementioned solvation effects. The mean energy gain due to the complex formation between **1** and one DMSO molecule was estimated to be in the range of 46.1 kJ/mol. However, the heat of vaporization of DMSO is equal to 43.1 kJ/mol (ref. 6). It should be noted that this value is very comparable to the calculated energy of the **1***DMSO adduct formation. Therefore, it is hardly possible to expect the formation of any long-living complexes of **1** with DMSO.

While studying the structure of the transition state for the NH₂ group rotation in compound **1** solvated by two DMSO molecules, some very similar effects were revealed: elongation of the N-H bond by 0.013-0.026 Å and shortening of the C-N bond by 0.027 Å. The energy barrier for amine group rotation becomes 8.1 kJ/mol higher, which is translated to about 30 times slower exchange of NH₂ protons at room temperature. An exchange of the NH₂ protons in CDCl₃ is evident from the broad signals at ~6.26 ppm (badly resolved doublet) in the experimental ¹H NMR spectrum of **1**. The mean calculated chemical shift of the NH₂ protons in the non-solvated molecule of **1** corresponds to ~5.86 ppm, which agrees reasonably well with the experimental value.

Several forms of solvates of compound **1** with two DMSO molecules were investigated. The calculations revealed that solvation of **1** with DMSO induces a significant (by 3-4 ppm) low-field shift of the NMR signals corresponding to the NH₂ protons. The mean value of the calculated chemical shifts of two NH₂ protons lies in the range between 10.6 and 10.8 ppm for the solvate, which agrees well with the experiment. Indeed, the ¹H NMR spectrum for compound **1** dissolved in DMSO shows two distinct peaks at 8.61 and 9.23 ppm for NH₂ protons, thus implying a low-field shift by >3 ppm as compared to the CDCl₃ solution (6.26 and 6.27 ppm).

It is interesting to mention that there is another isomer of **1** with additional cycle formed via formal conjugation of the NH₂ and adjacent CN groups leading to the formation of N-N bond (Fig. S23). This isomer lies only 15.7 kJ/mol higher in energy than the ground isomer **1**, but, apparently, there is no chemical pathway for their facile interconversion.

References

1. J.P. Perdew, K. Burke, M. Ernzerhof, *Phys. Rev. Lett.* **1996**, *77*, 3865-3868.
2. D.N. Laikov, *Chem. Phys. Lett.*, **2005**, *416*, 116 - 120.
3. D.N. Laikov, *Chem. Phys. Lett.*, **1997**, *281*, 151 - 156.
4. E.D. Raczyńska, T.M. Stępniewski, K.Kolczyńska, *J. Mol.Model.* **2011**, *17*, 3229–3239.
5. E.D. Raczyńska, T.M. Stępniewski, K.Kolczyńska, *J. Mol.Model.* **2012**, *18*, 4367–4380.
6. D. R. Lide CRC Handbook of Chemistry and Physics 85th edition. CRC Press, 2004.

Fabrication and characterization of the OFET-based memory elements using compound **5** as a light-sensitive component

Glass slides (15x15 mm) were cleaned by sonication in a base piranha solution (a mixture of hydrogen peroxide and ammonia, both obtained from ChimMed, Russia), rinsed with deionized water, dried in an oven at 60°C for 30 min. Aluminium gate electrodes with a thickness of 200 nm were deposited by thermal evaporation in vacuum (8×10^{-6} mbar) in nitrogen glove box through a shadow mask. The dielectric layer of AlO_x (~10 nm) was grown by anodic oxidation of aluminum gate electrodes in 0.01 mol citric acid (Acros Organics) at a constant potential of 18 V. Afterwards, the samples were rinsed with deionized water and dried at 60 °C for 15 min. Triazaphenalene **5** was spin-coated from the DMF solution (10 mg/mL) on the top of the AlO_x dielectric at 1000 rpm inside a nitrogen glove box. Then the samples were transferred to the vacuum chamber (also integrated inside glove box) and [60]fullerene semiconductor layer (100 nm) was grown by thermal evaporation in high vacuum (2×10^{-6} mbar) with the rate of 0.5-0.8 Å/s at 280 °C. The devices were completed by deposition of the 100 nm thick silver source and drain electrodes through a shadow mask. The channel length (L) and width (W) were 75 and 2000 μm, respectively.

The electrical characterization of the devices was performed using double-channel Keithley 2612A source-measurement unit. Programming of the memory elements was achieved by applying constant electric bias ($V_p = 5$ V) between source and gate electrodes of the device (writing regime) or simultaneous application of $V_p = -10$ V and illumination of the OFET channel with violet light ($\lambda = 405$ nm, $P \sim 60$ mW/cm²) for 0.5 s (erasing regime). The laser was modulated using programmable Advantest R6240A DC voltage current source/monitor. Full transfer characteristics

of the transistors and/or drain currents at constant drain and gate voltages were registered after each programming step.

Fabrication and characterization of OLEDs based on compound 1

The patterned ITO-coated glass substrates were sonicated consecutively with acetone and iso-propyl alcohol for 10 min. PEDOT:PSS (Baytron PH-100) was spin-coated at 1500 rpm to produce ca. 50 nm thick film. The PEDOT:PSS films were dried inside argon glove box for 30 min at 200 °C. Afterwards, thin films of 2-TNATA (60 nm), NPD (20 nm) and compound **1** (30 nm) were thermally evaporated in high vacuum (10^{-6} mbar). The device layer stack was completed by depositing calcium top electrodes (100 nm).

Current-voltage characteristics of OLEDs were measured using Keithley 2400 source-measurement unit. Brightness and EL spectra of the devices were obtained using calibrated Avantes AvaSpec-2048 spectrometer operating in a radiometry regime.

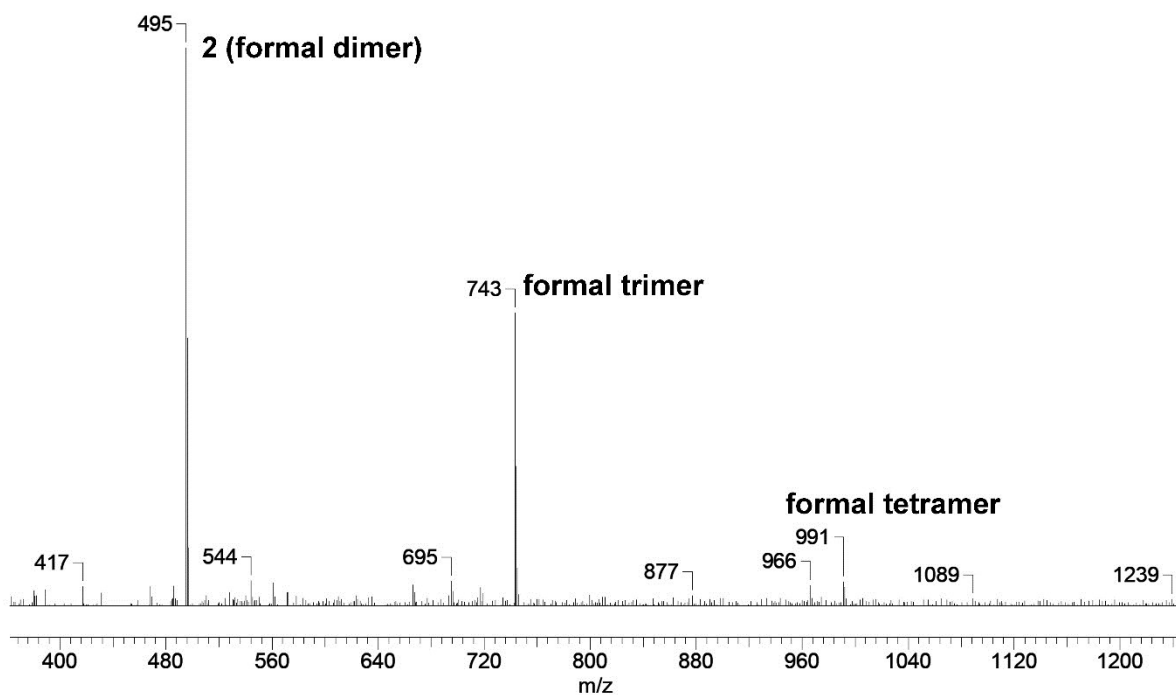
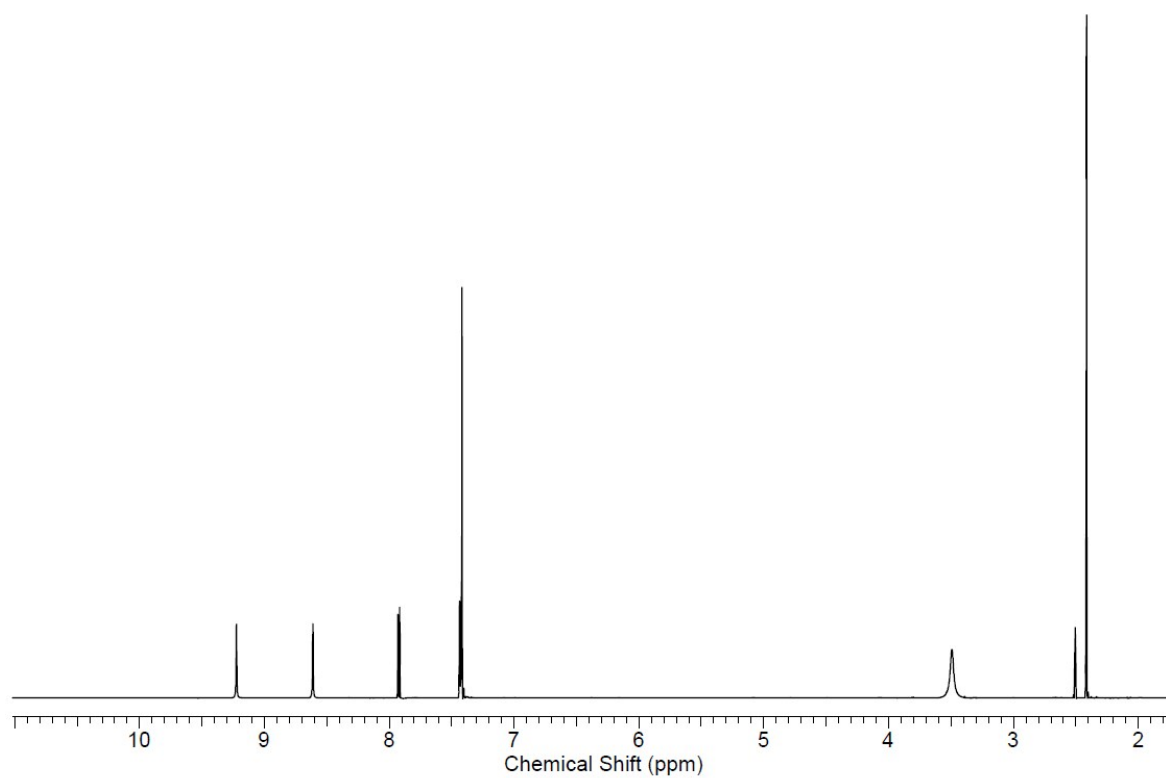


Figure S1. ESI mass spectrum of the crude reaction product formed *via* thermal cyclization of 3-(4-methoxyphenyl)cyclopropane-1,1,2,2-tetracarbonitrile, showing the formation of triazaphenalene **2** as a major (formal dimerization) product along with the unidentified cyclopropane trimerization and tetramerization products.

a



b

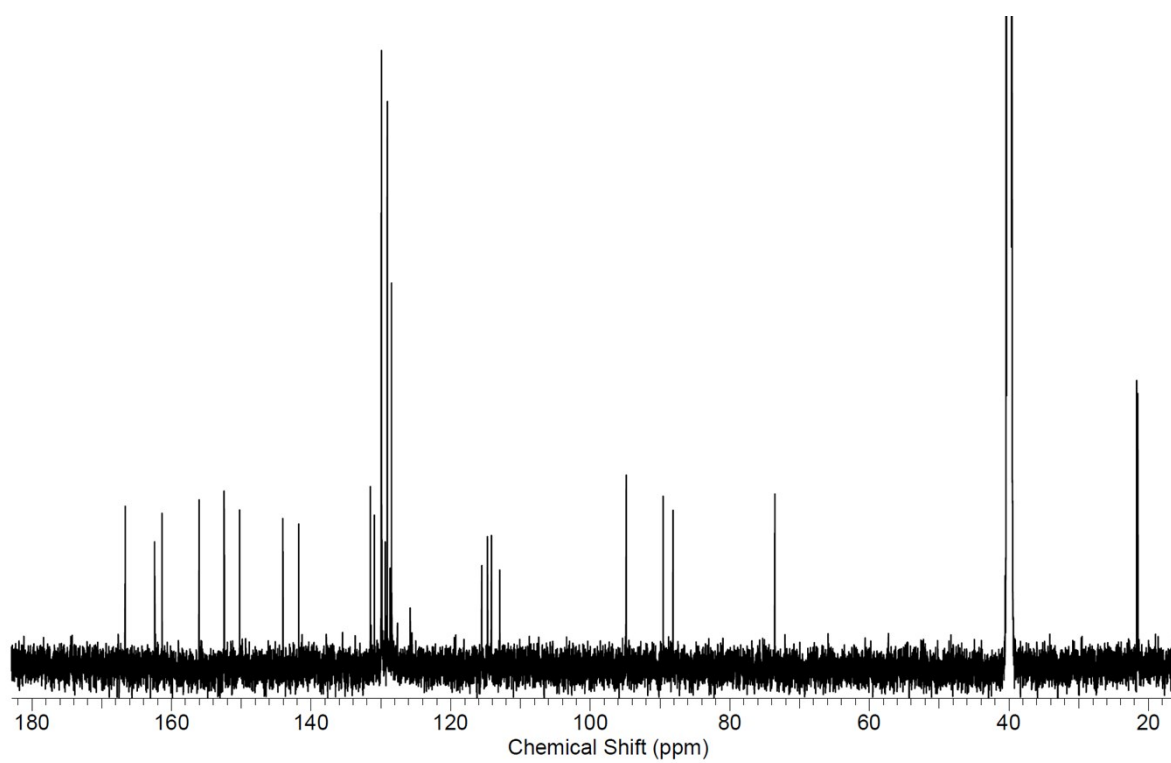


Figure S2. ^1H (a) ^{13}C (b) NMR spectra of compound **1** recorded in DMSO-D_6

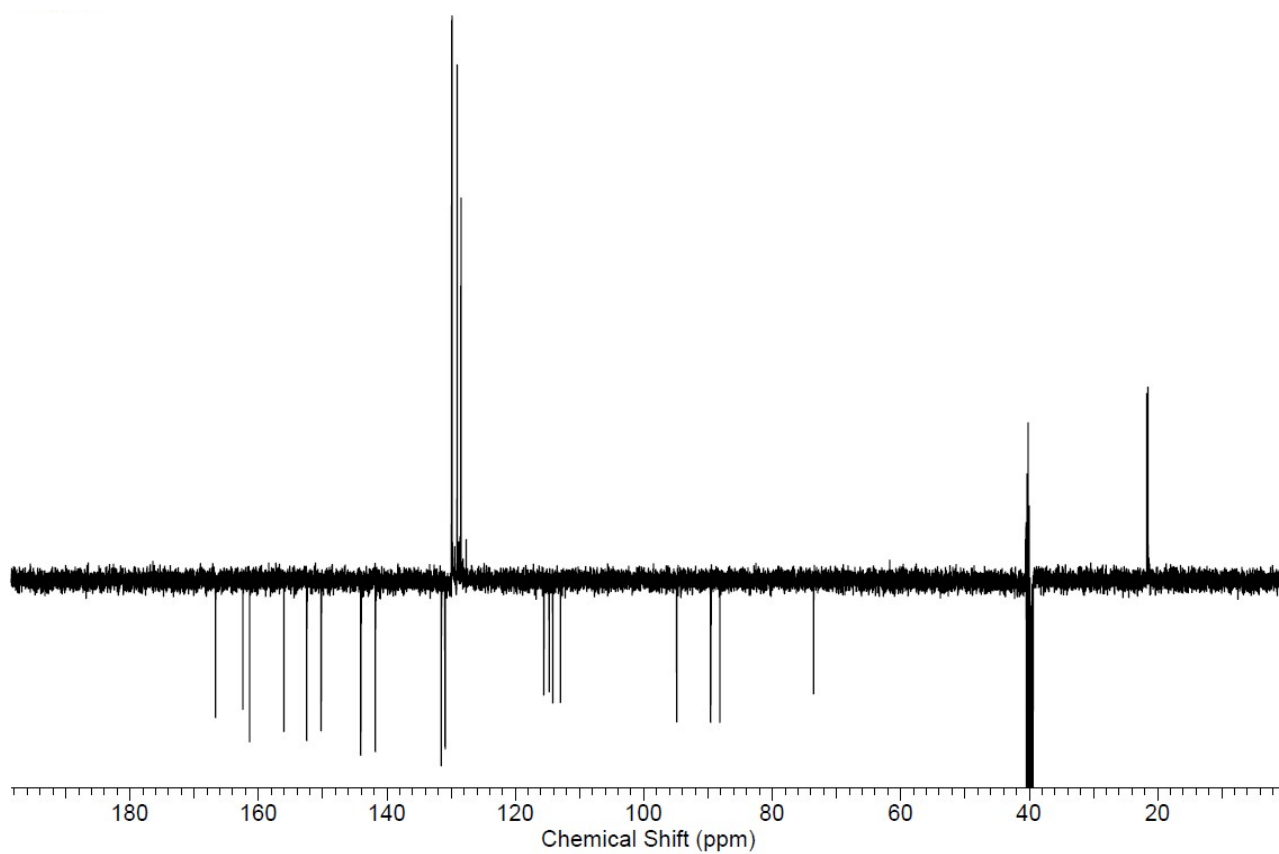


Figure S3. J-mode ^{13}C NMR spectrum of compound **1** recorded in DMSO-D_6

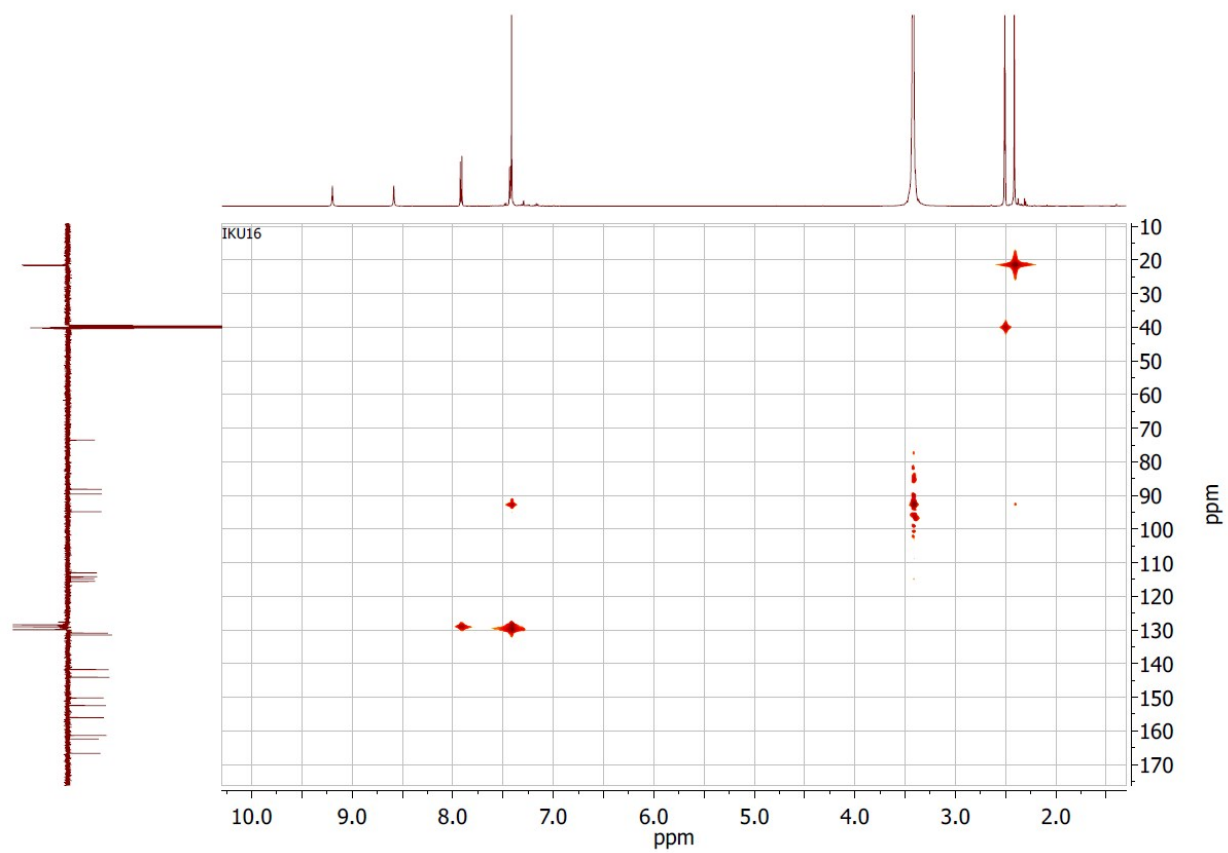


Figure S4. 2D H-C HSQC NMR spectrum of **1** in DMSO-D_6

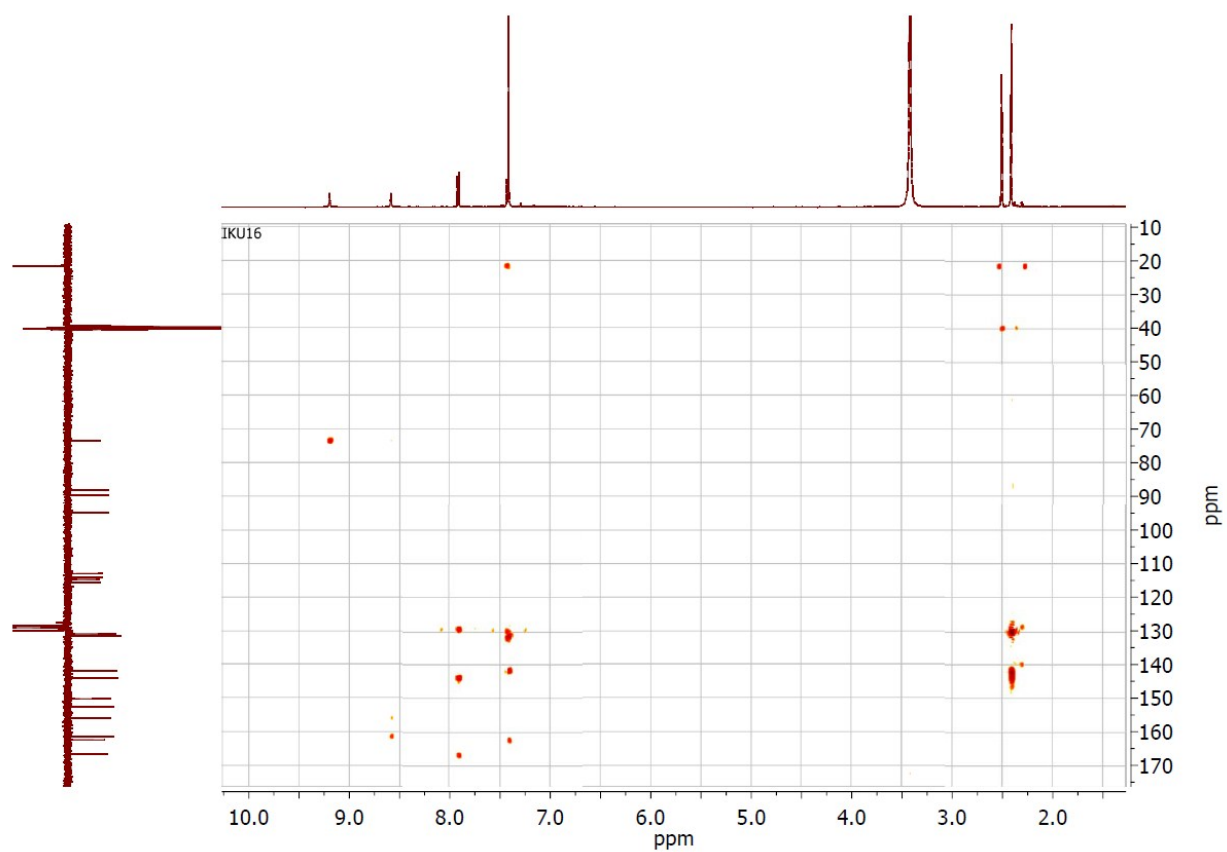


Figure S5 2D H-C HMBC NMR spectrum of **1** in DMSO-D₆

sd43.3_001001r

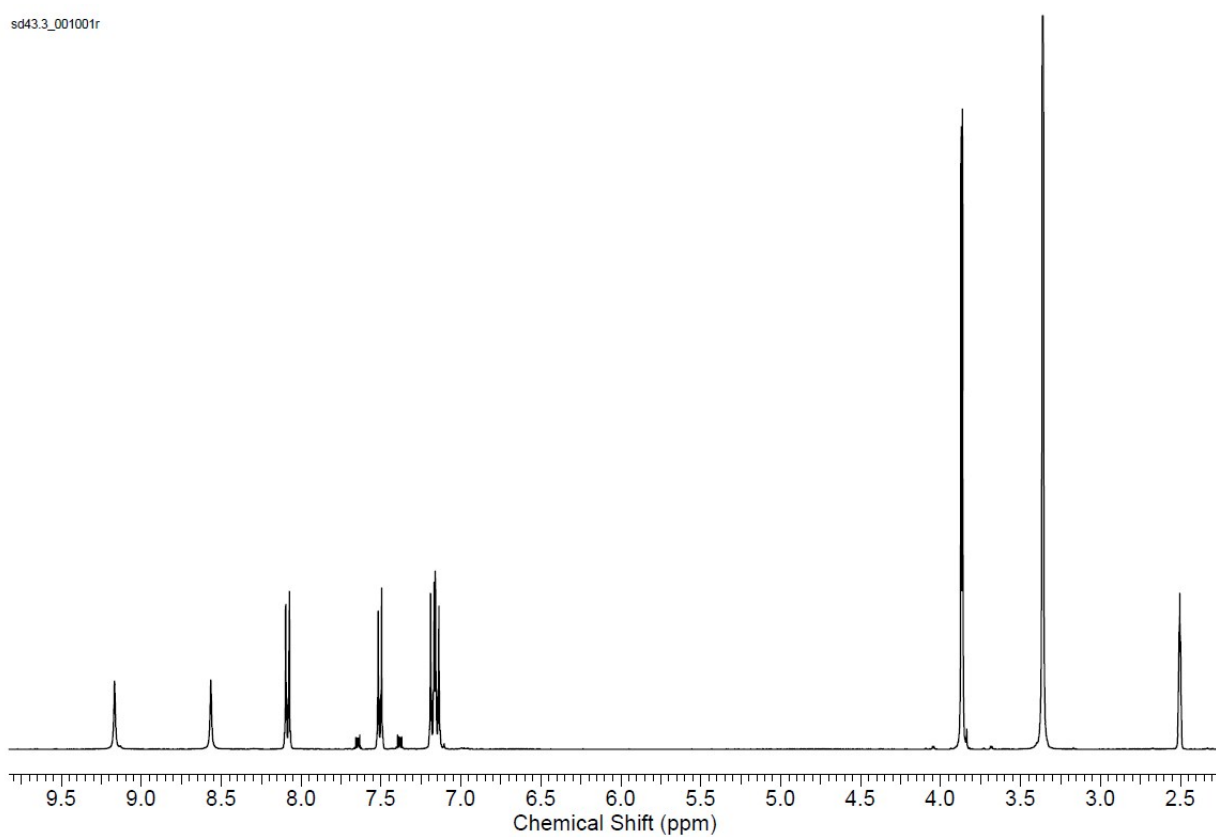


Figure S6. ^1H NMR spectrum of **2** in DMSO-D_6

sd43.3_132001r

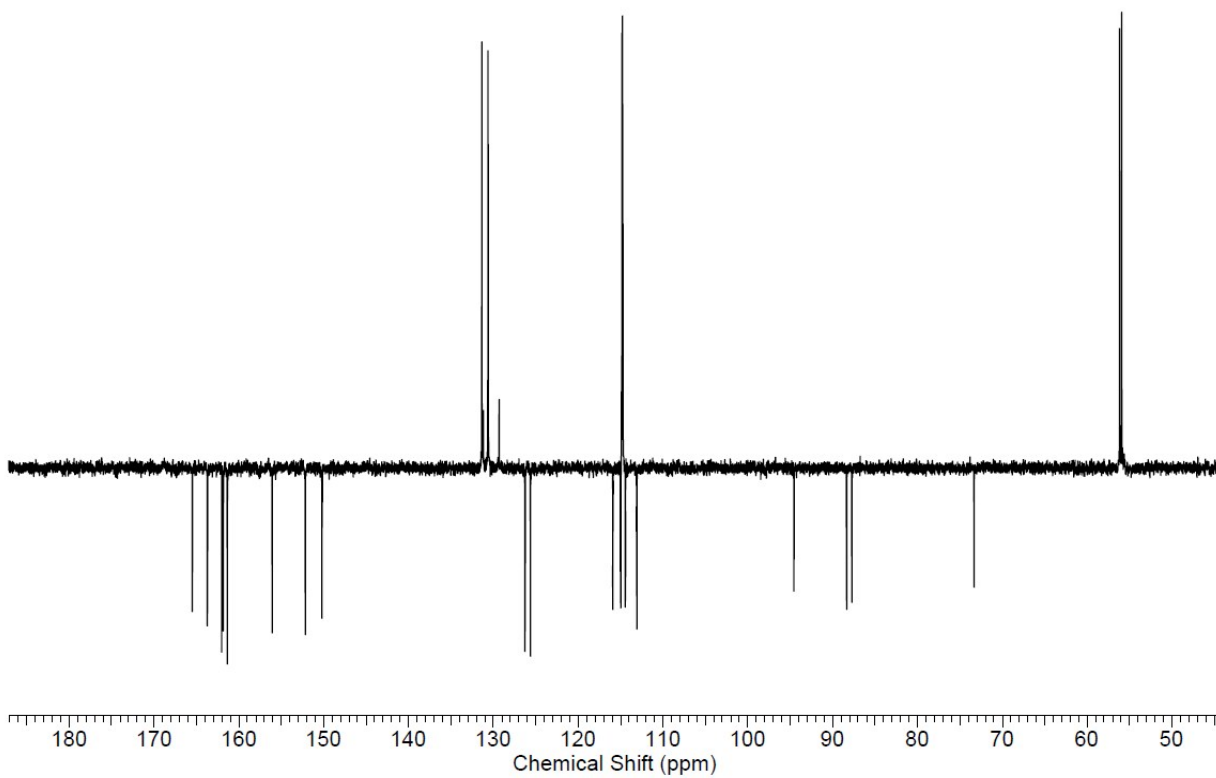


Figure S7. J-mode ^{13}C NMR spectrum of **2** in DMSO-D_6

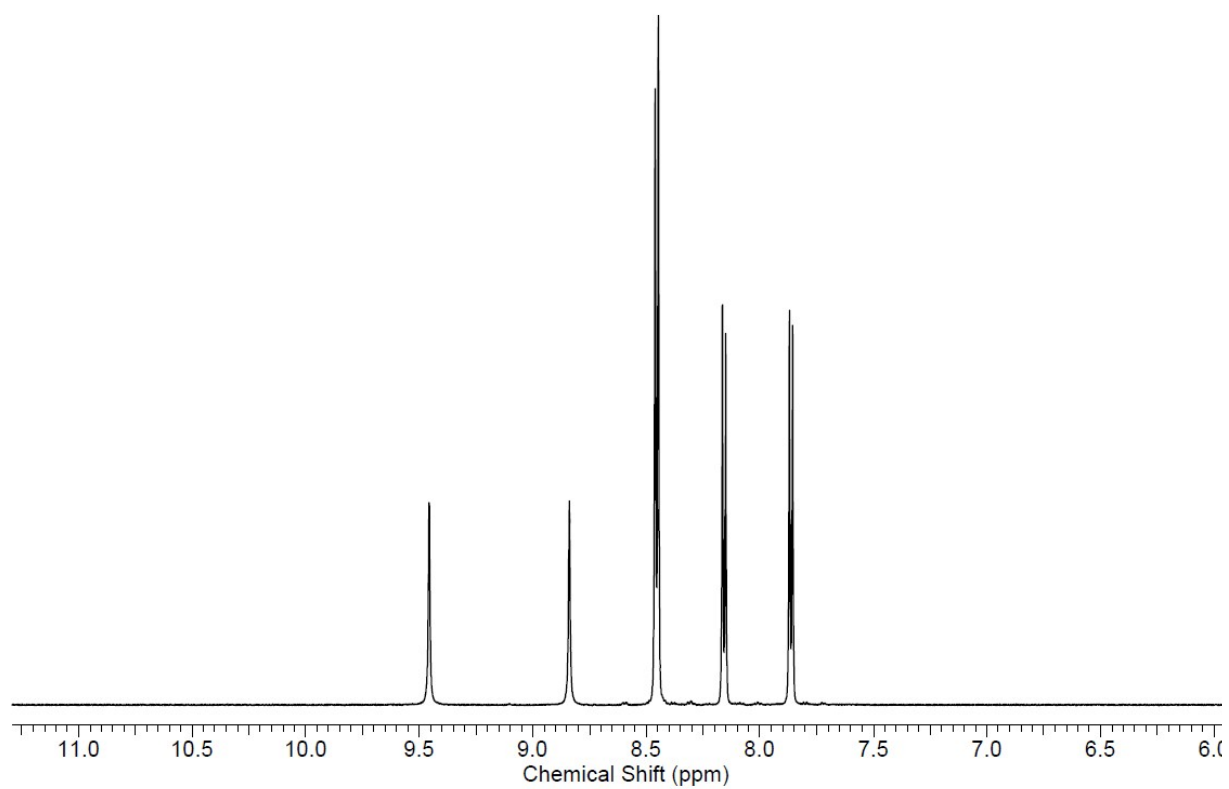


Figure S8. ^1H NMR spectrum of **3** in DMSO-D_6

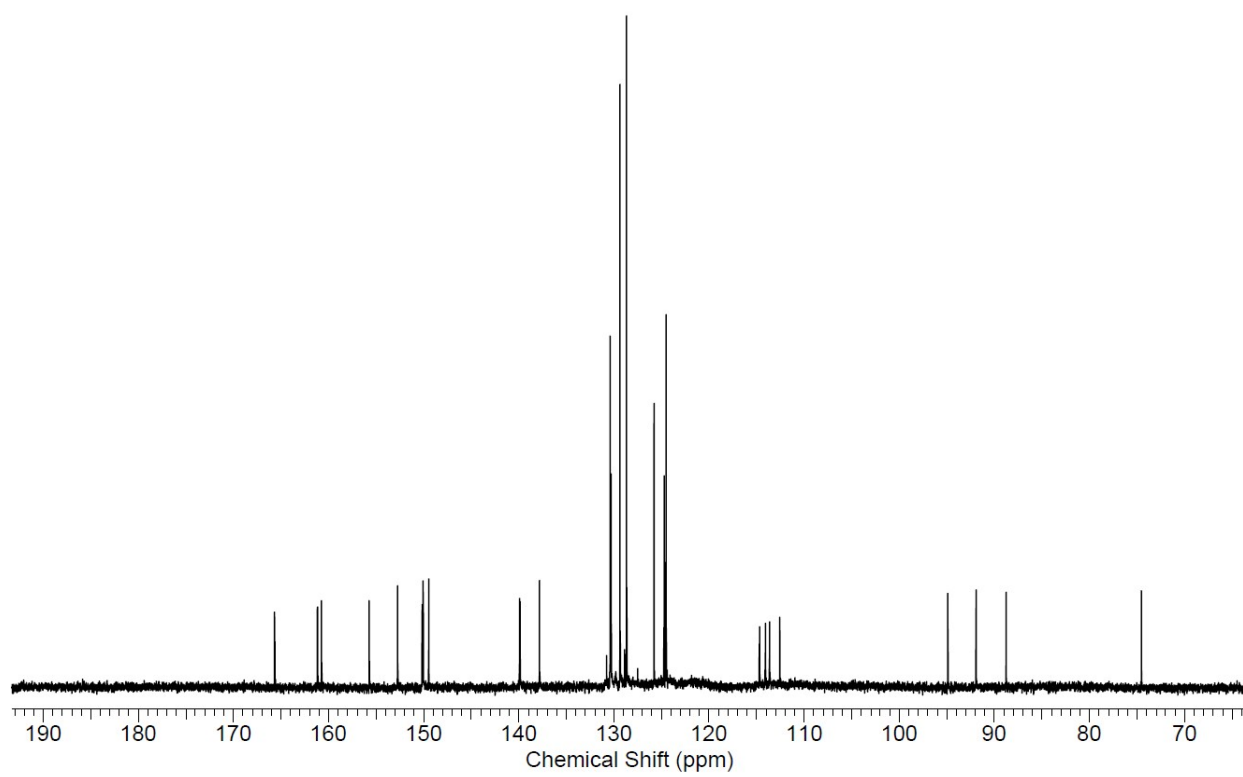


Figure S9. ^{13}C NMR spectrum of **3** in DMSO-D_6

IKU32_001001r.esp

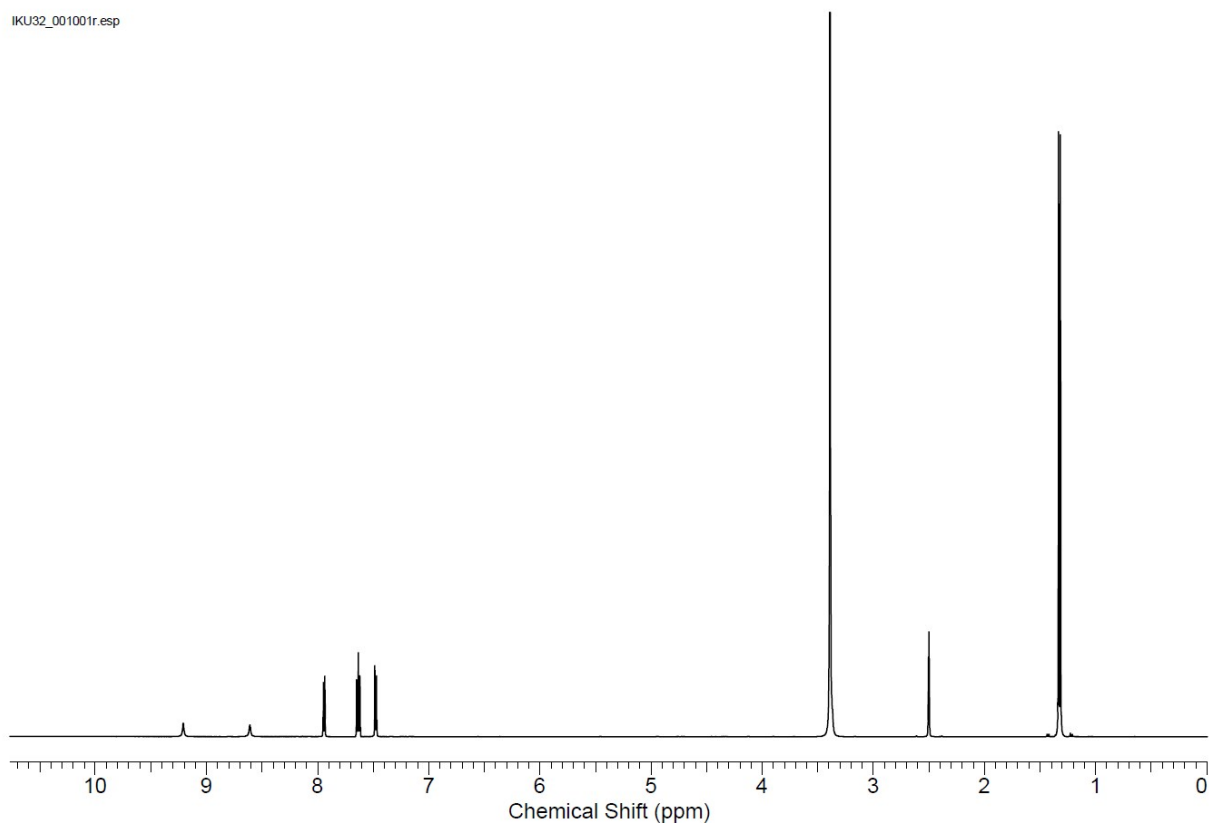


Figure S10. ^1H NMR spectrum of **4** in DMSO-D_6

IKU32_001001r.esp

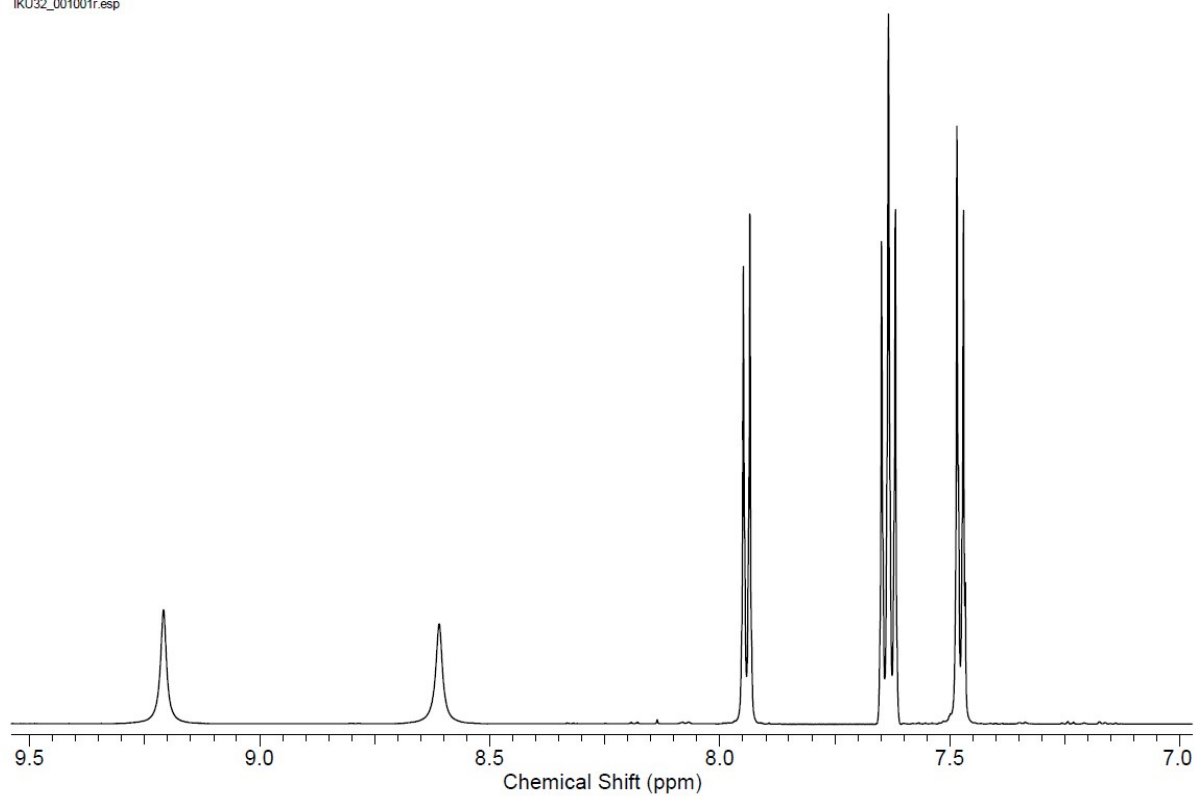


Figure S11. A low-field part of ^1H NMR spectrum of **4** in DMSO-D_6

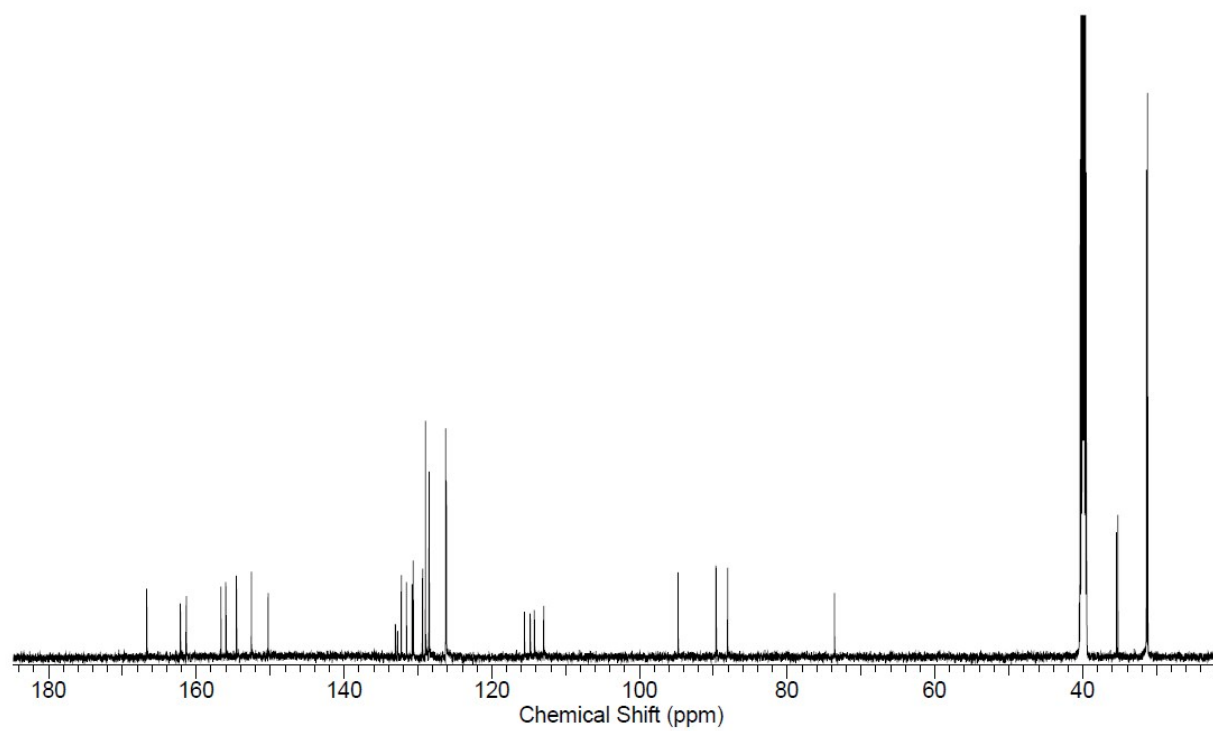


Figure S12. ^{13}C NMR spectrum of 4 in $\text{DMSO-}D_6$

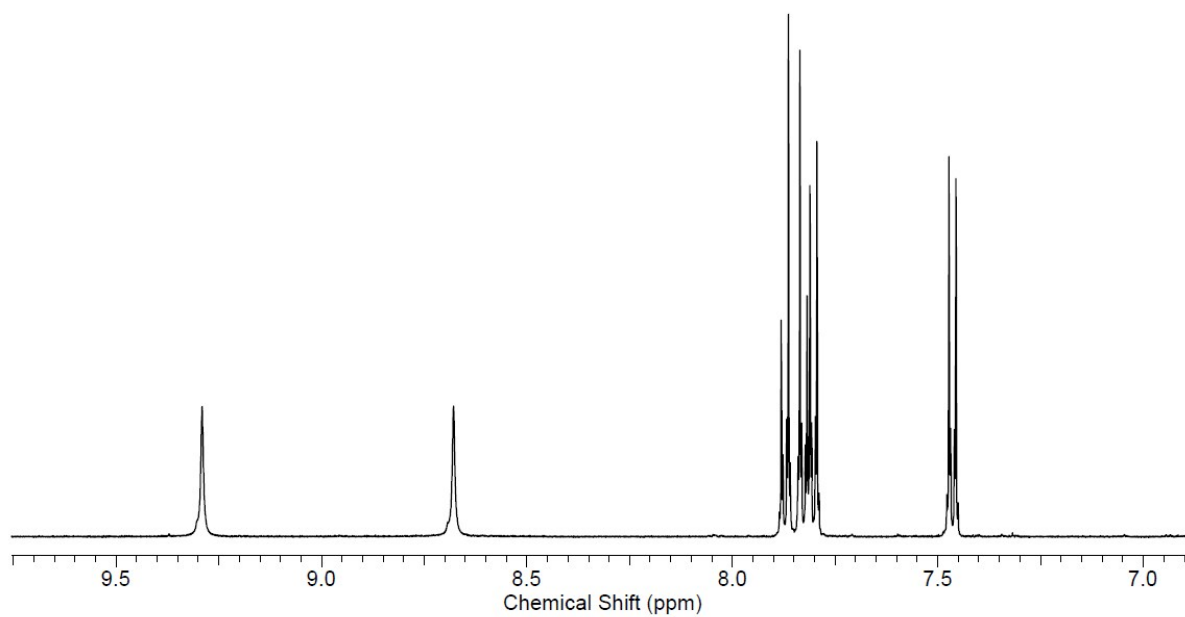


Figure S13. ^1H NMR spectrum of **5** in DMSO-D_6

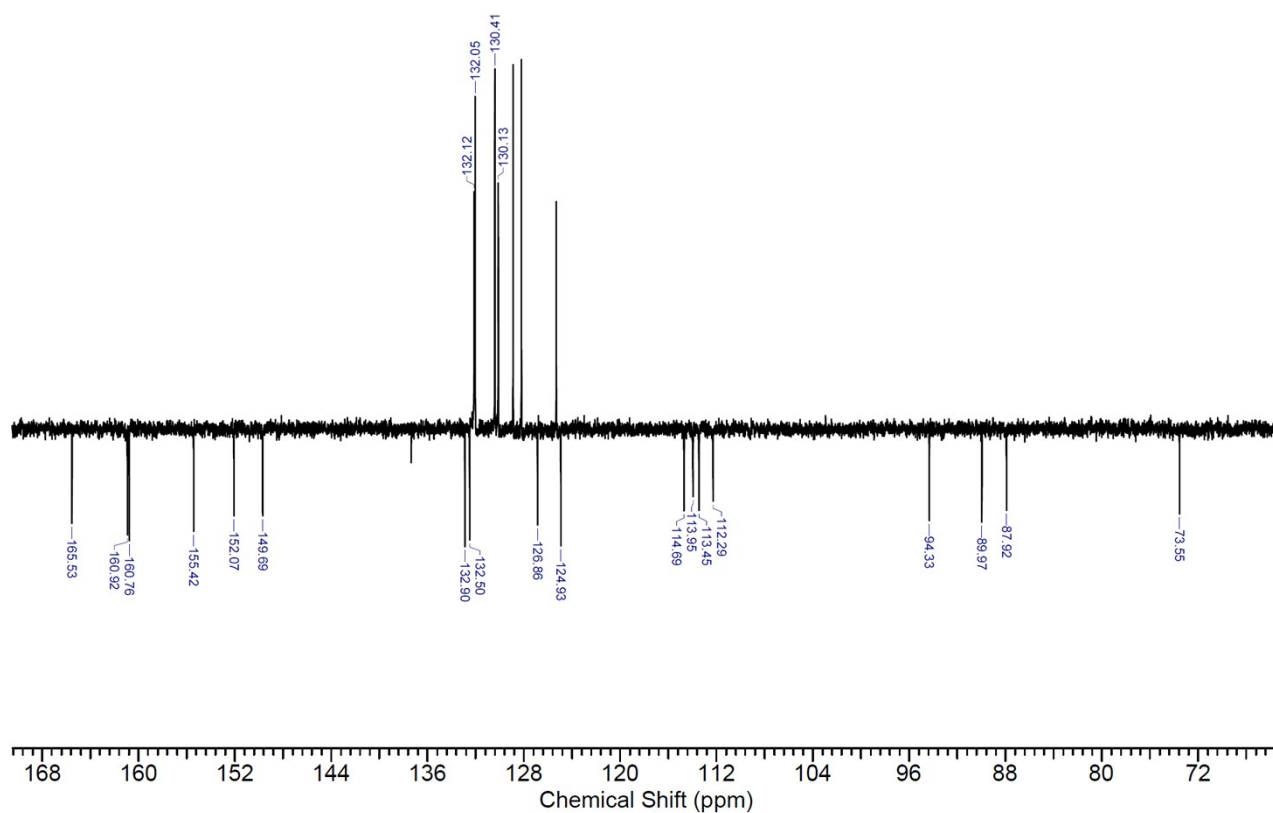


Figure S14. ^{13}C NMR spectrum of **5** in DMSO-D_6 (four unlabeled peaks correspond to the toluene impurity appearing due to the stable solvate formation with compound **5**)

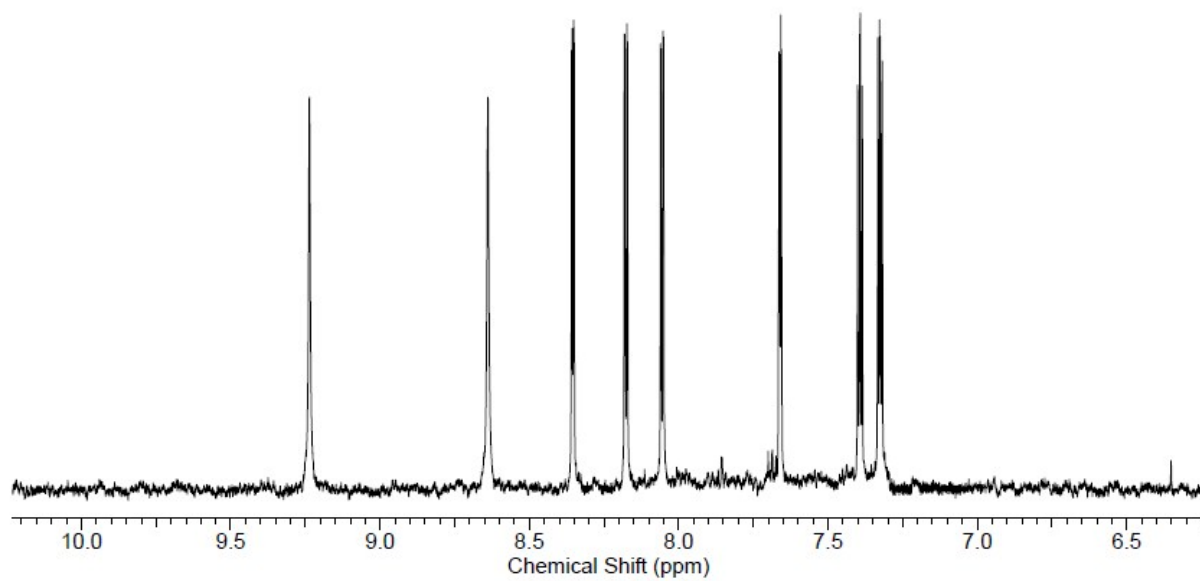


Figure S15. ^1H NMR spectrum of **6** in DMSO-D_6

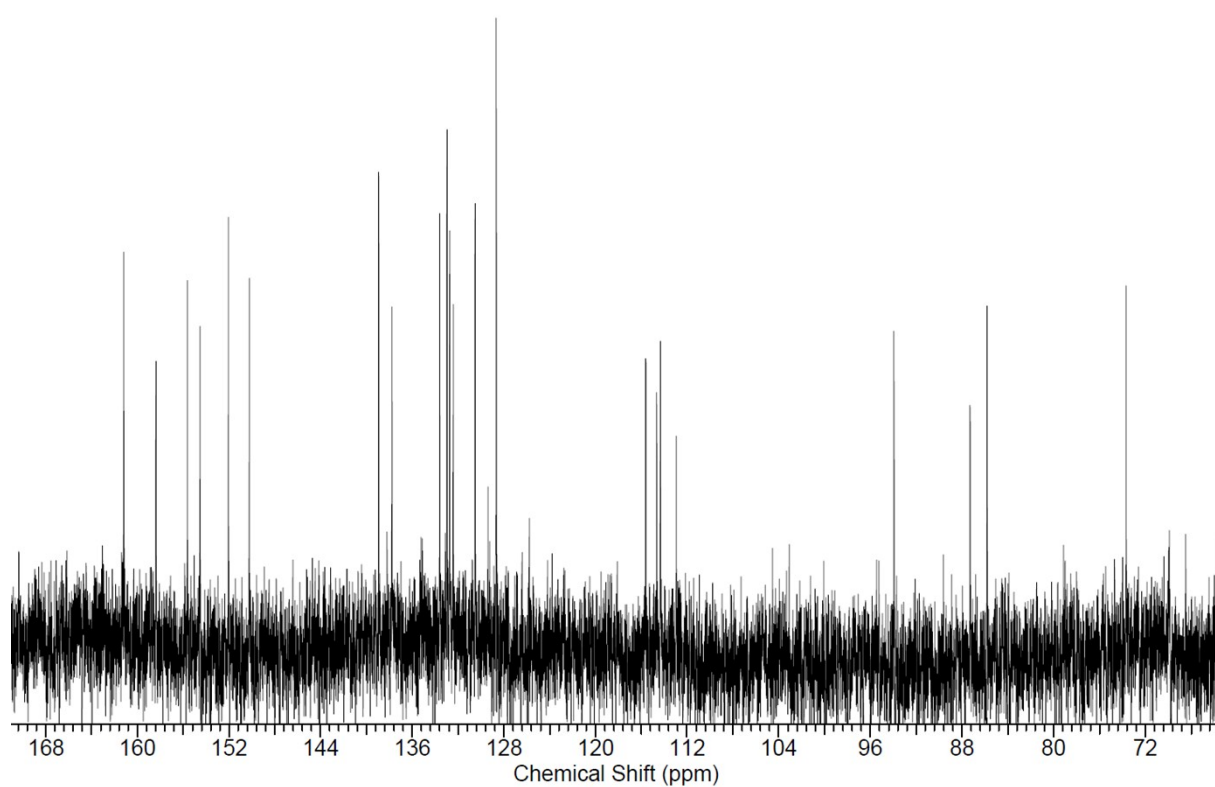
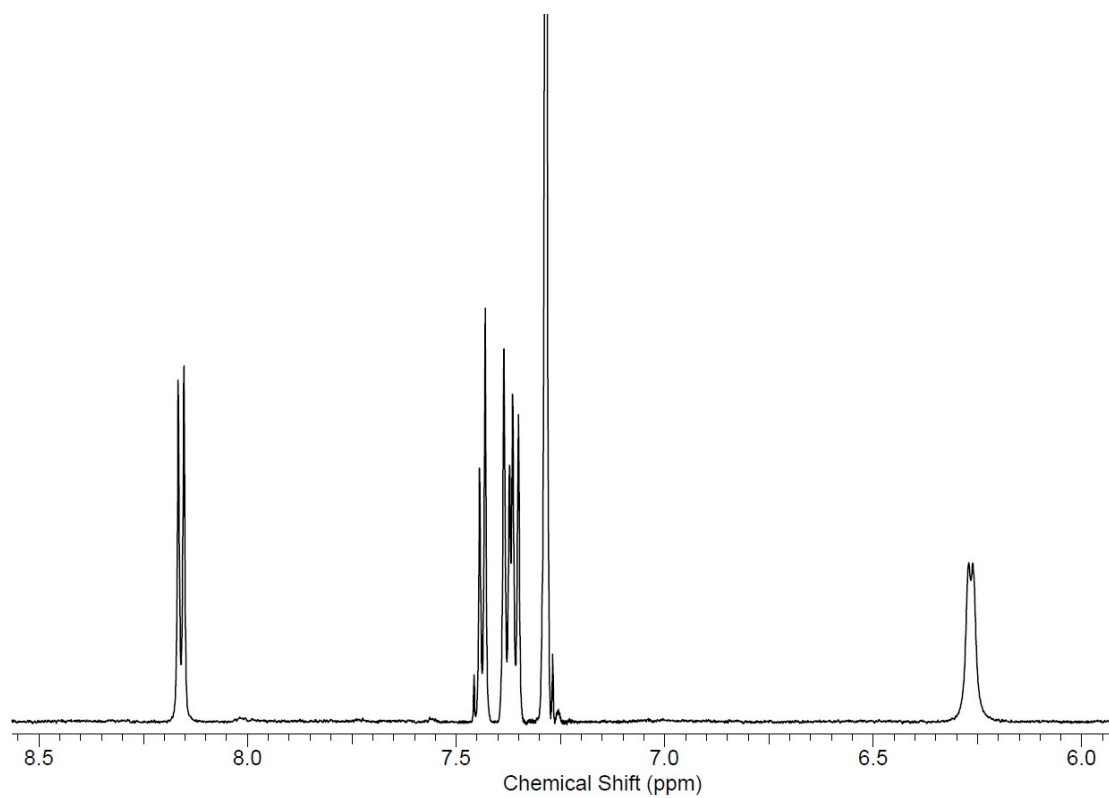


Figure S16. ^{13}C NMR spectrum of **6** in DMSO-D_6

a



b

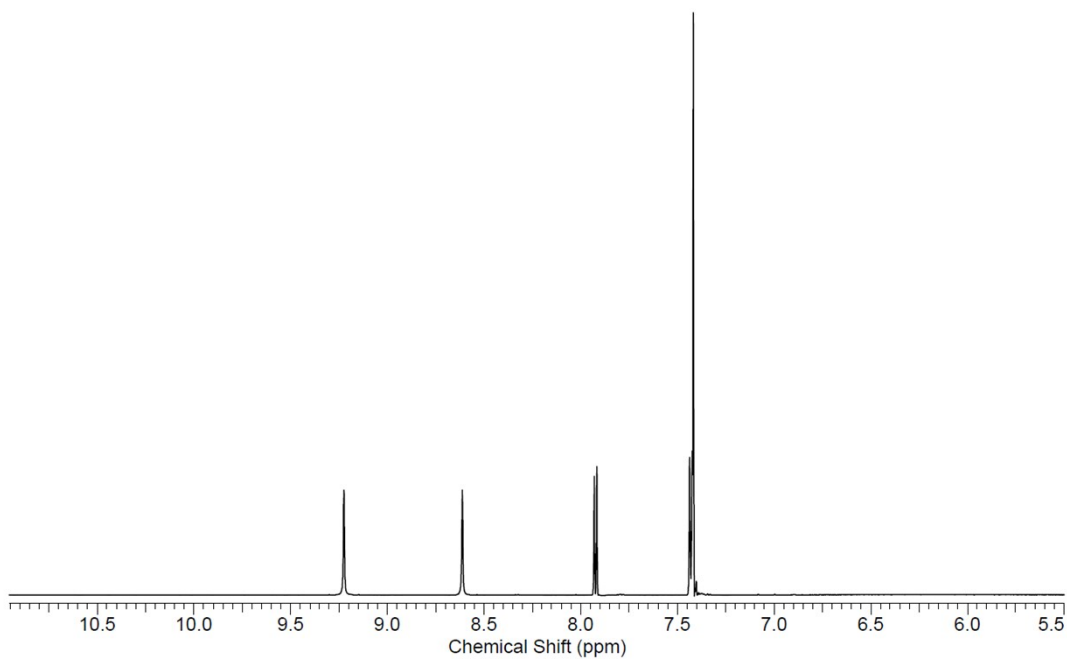


Figure S17. Low-field parts of the ^1H NMR spectra of **1** in CDCl_3 (a) and DMSO-D_6 (b)

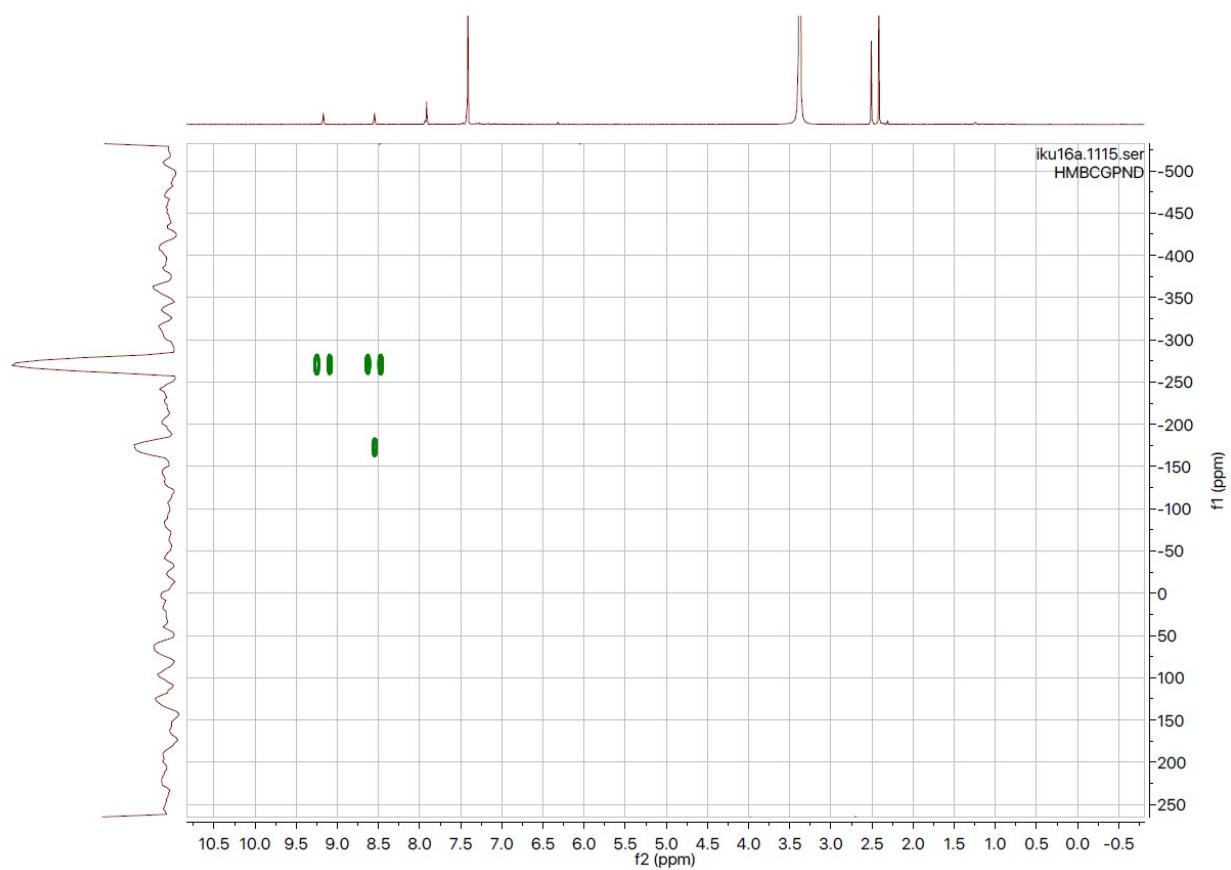


Figure S18. 2D ^1H - ^{15}N HMBC spectrum of compound **1** in DMSO- D_6

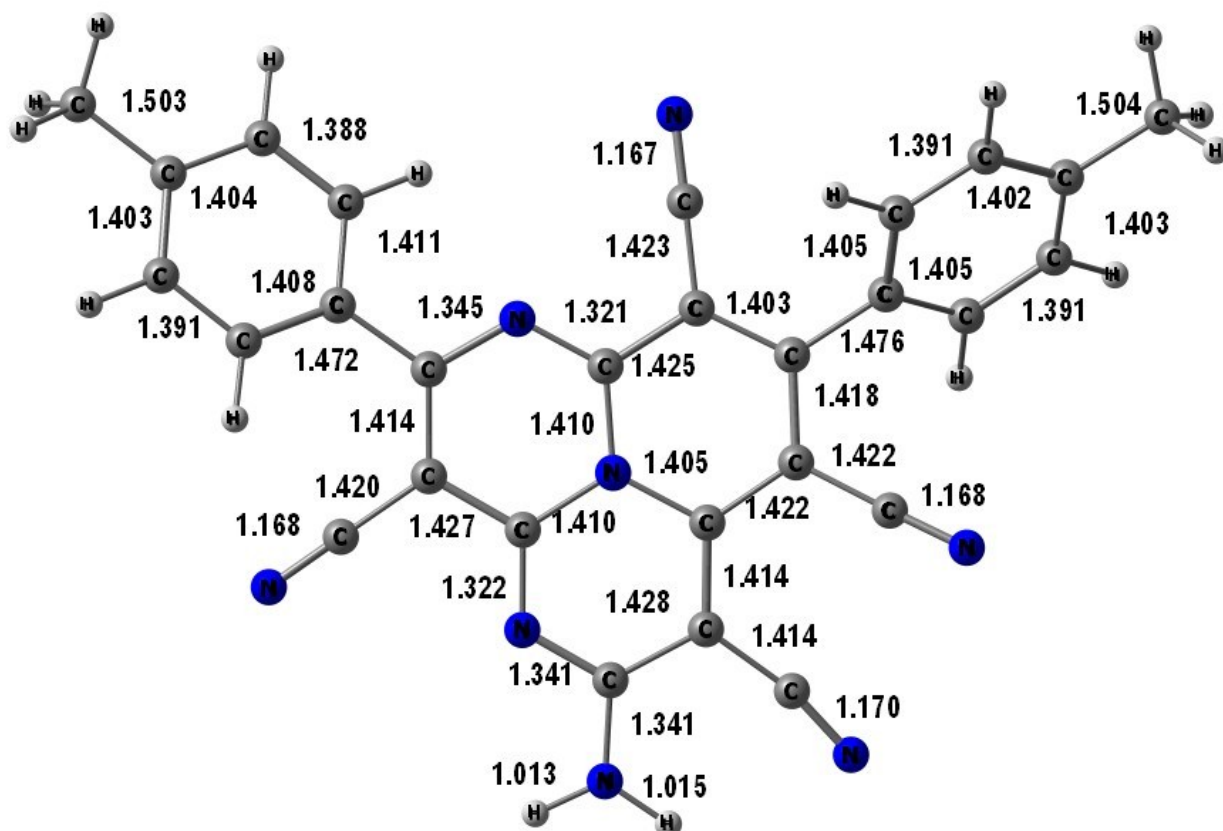


Figure S19. Calculated molecular structure of compound **1**.

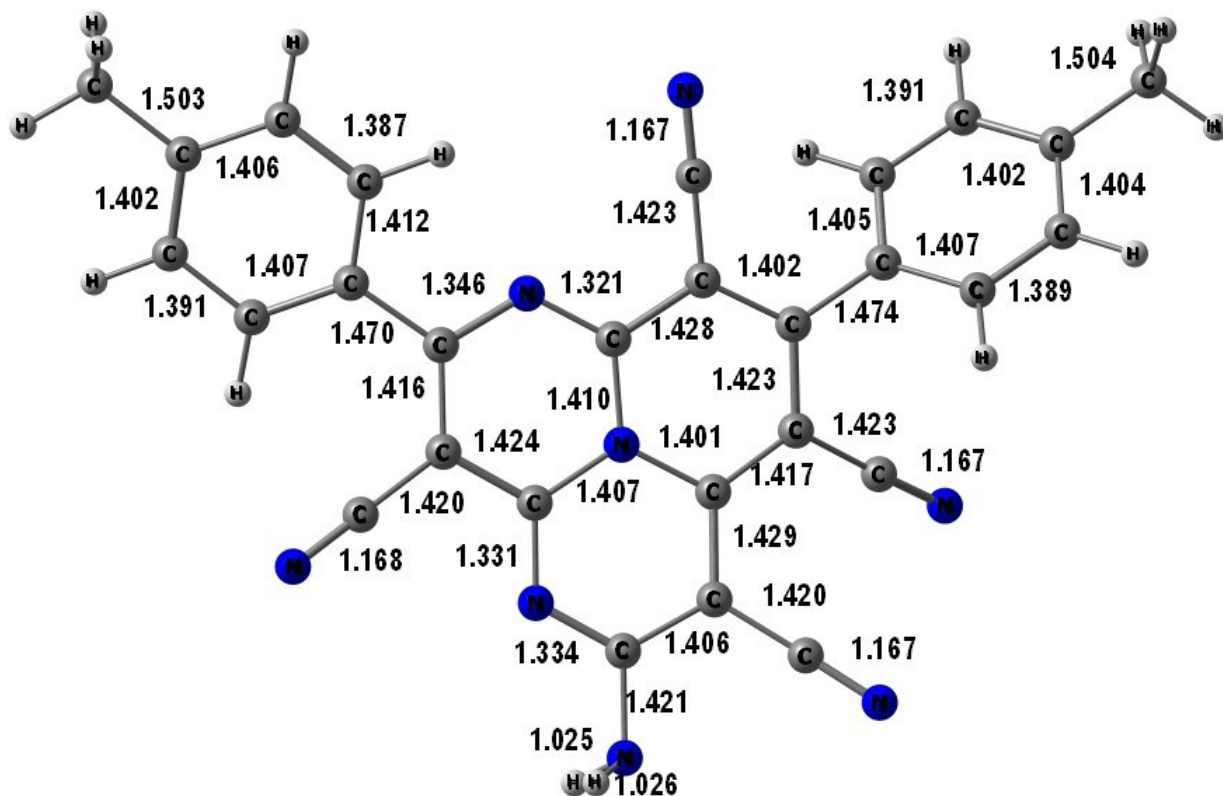


Figure S20. Calculated structure of the transition state for rotation of NH_2 group in **1**.

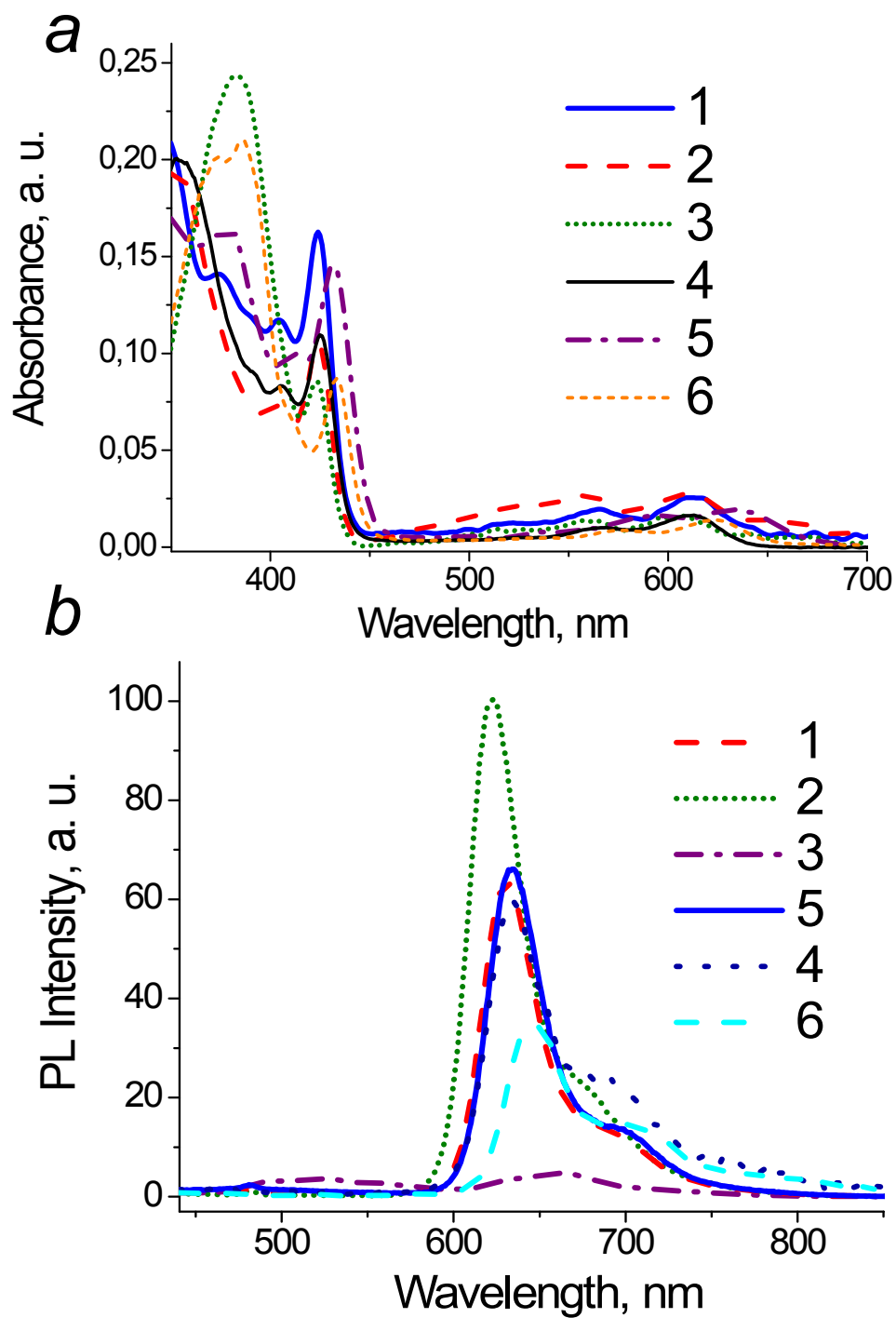


Figure S21. Absorption and PL spectra of selected triazaphenalenenes **1-6** in toluene solutions

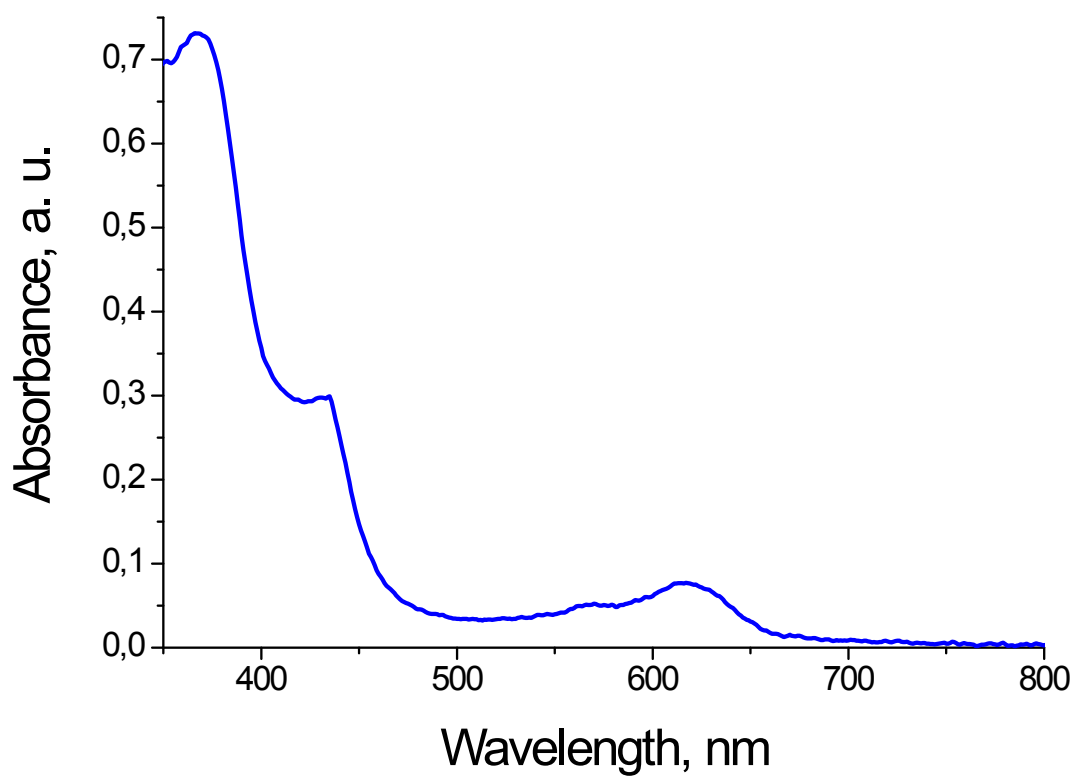


Figure S22. Solid-state absorption spectrum of triazaphenalene 1

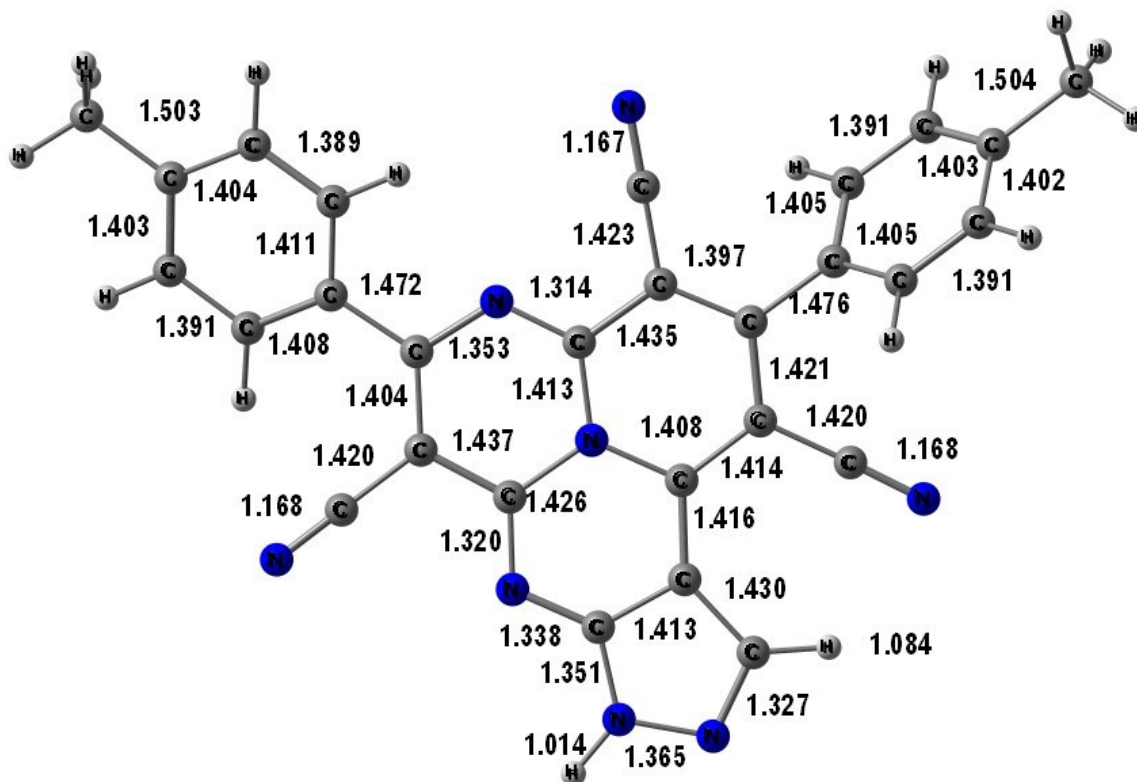


Figure S23. Calculated structure of the product of cyclization of 1.